



EUROPEAN  
COMMISSION

Community research



## Long-term Performance of Engineered Barrier Systems PEBS

### Engineered Barrier Emplacement Experiment in Opalinus Clay: “EB” Experiment

### Geoelectrical monitoring of dismantling operation

### (DELIVERABLE-N°: D2.1-9)

Contract (grant agreement) number: FP7 249681

Author(s):

Markus Furche, Kristof Schuster

Date of issue of this report: 05/03/2014

Start date of project: 01/03/10

Duration : 48 Months

<b>Project co-funded by the European Commission under the Seventh Euratom Framework Programme for Nuclear Research &amp; Training Activities (2007-2011)</b>		
<b>Dissemination Level</b>		
<b>PU</b>	Public	<b>PU</b>
<b>RE</b>	Restricted to a group specified by the partners of the [acronym] project	
<b>CO</b>	Confidential, only for partners of the [acronym] project	

PEBS



# Table of Contents

<b>1</b>	<b>Introduction .....</b>	<b>4</b>
1.1	The EB project .....	4
1.2	Background.....	6
1.2.1	Funding .....	6
1.2.2	Experiment development.....	6
1.3	Reactivation of an installed electrode array .....	8
<b>2</b>	<b>Method .....</b>	<b>8</b>
2.1	Fundamentals of DC Geoelectrics.....	8
2.2	Inversion .....	10
<b>3</b>	<b>Field Measurements.....</b>	<b>11</b>
3.1	Hardware and setup .....	11
3.2	Monitoring period.....	12
3.3	Layout .....	13
3.4	Configurations and inversion .....	14
<b>4</b>	<b>Results and Conclusion.....</b>	<b>16</b>
4.1	Situation before dismantling operation.....	16
4.1.1	Comparison with results from pilot borehole .....	17
4.1.2	Comparison with results from sample analysis .....	18
4.2	Situation after finished dismantling operation .....	20
4.2.1	Comparison to a stress analysis.....	21
<b>5</b>	<b>Summary.....</b>	<b>21</b>
<b>6</b>	<b>References.....</b>	<b>22</b>

## List of figures

Figure 1: EB experimental layout.....	5
Figure 2: Principle of resistivity measurement with a four-electrode array (after Knödel et al., 2007).....	8
Figure 3: Setup for a 2D resistivity measurement (imaging) using a Wenner- $\alpha$ electrode configuration and presentation as a pseudosection (modified after Knödel et al., 2007).....	10
Figure 4: Pictures of the experimental setup; left: test measurement, laptop controlled; right: installation in an aluminum box for monitoring, device controlled.....	12
Figure 5: Sketch of the three electrode profiles installed in the EB niche in 2001 (Kruschwitz & Yaramanci, 2002).....	13
Figure 6: Contact resistances of all electrodes of circular profile 2 on July 4 <sup>th</sup> , 2012.....	14
Figure 7: Geometry of EB niche including concrete bed and dummy canister with electrode positions.....	14
Figure 8: Model of the spatial resistivity distribution on September 30 <sup>th</sup> 2012.....	16
Figure 9: Result of the geoelectrical profile measurements in the pilot borehole.....	17
Figure 10: Position of sampling sections and the used circular profile.....	18
Figure 11: Spatial distribution of water content at section “E” and “B2” as a result of sample analysis while dismantling (from Palacios et al., 2013).....	18
Figure 12: Positions of samples (section “E”) for laboratory investigations.....	19
Figure 13: Resistivity as a function of water content of 6 bentonite samples.....	20
Figure 14: Resistivity distribution in the Opalinus Clay around the EB niche at 2 distinct time steps after finished dismantling; left: February 16 <sup>th</sup> 2013, right: Mai 23 <sup>th</sup> 2013.....	20
Figure 15: Spatial stress distribution in the environment of the EB niche (Corkum, 2006).....	21

# **1 Introduction**

The following introduction particularly the sections 1.1 and 1.2 is geared to the PEBS Deliverable D2.1-4 by Palacios et al. (2013). Section 1.2.2 is completed by some additional geophysical and geotechnical aspects.

## **1.1 The EB project**

The Engineered Barrier Emplacement Experiment in Opalinus Clay “EB” Experiment aimed the demonstration of a new concept for the construction of HLW repositories in horizontal drifts, in competent clay formations. The principle of the new construction method was based on the combined use of a lower bed made of compacted bentonite blocks, and an upper buffer made of granular bentonite material (GBM). The project consisted on a real scale isothermal simulation of this construction method in the Opalinus Clay formation at the Mont Terri underground laboratory in Switzerland. A steel dummy canister, with the same dimensions and weight as the Spanish reference canister, was placed on top of a bed of bentonite blocks, and then the upper part of the drift was buffered with the GBM made of bentonite pellets (Figure 1). The drift was sealed with a concrete plug having a concrete retaining wall between the plug and the GBM. Since the end of the test installation the evolution of the different hydro-mechanical parameters were being monitored, both in the barrier and the rock (especially in the Excavation Disturbed Zone (EDZ)). Relative humidity and temperature in the rock and in the bentonite buffer, rock displacement, pore pressure and total pressure were registered by means of different types of sensors. Due to the short amount of free water available in this formation, an artificial hydration system was installed to accelerate the hydration process in the bentonite.

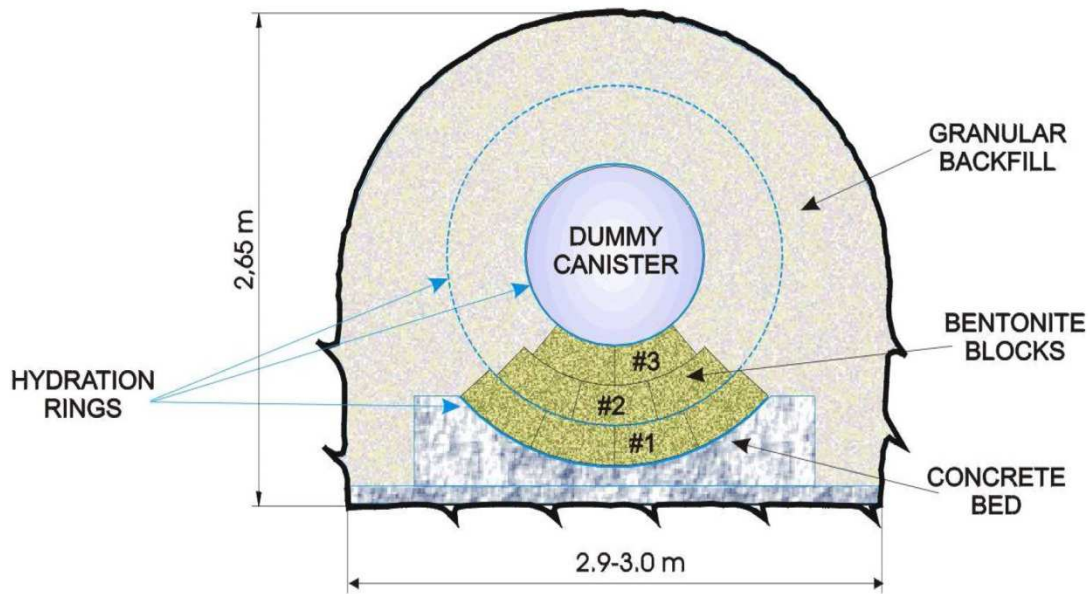


Figure 1: EB experimental layout

The basic objectives of the project were the following:

- Definition of backfill material (composition, grain size distribution ...). Demonstration of the manufacturing process at semi-industrial scale.
- Characterization of the hydro-mechanical properties of the backfill material.
- Design and demonstration of the emplacement and backfilling technique.
- Quality Assessment of the clay barrier in terms of the achieved geomechanical parameters (homogeneity, dry density, voids distribution ...) after emplacement.
- Characterization of the EDZ in the Opalinus Clay, and determination of its influence in the overall performance of the system.
- Investigation of the evolution of the hydro-mechanical parameters in the clay barrier and the EDZ as a function of the progress of the hydration process.
- Development of a hydro-mechanical model of the complete system adjusted and calibrated with the data resulting from the experiment.

After 11 years of operation, the experiment has been dismantled between the 19<sup>th</sup> of October 2012 and the 1<sup>st</sup> of February 2013. The aim of this document is to describe the design, results and conclusions of distinct time steps of the geoelectrical monitoring of the dismantling operation.

## **1.2 Background**

### **1.2.1 Funding**

The first phase of the EB experiment -years 2000 to 2003-, devoted to the test design, installation and start-up of the operation, was co-financed by the European Commission (contract n° FIKW-CT-2000-00017), under the framework of the research and training programme (Euratom) in the field of nuclear energy, and ENRESA (Spain). Besides ENRESA, BRG (Germany) and NAGRA (Switzerland) were the principal contractors and AITEMIN (Spain) and CIMNE (Spain) the assistant contractors.

Between 2003 and 2009 the project operation continued under the support of the Mont Terri Consortium, project 32.015: EB, phases 10 to 14.

From 2010, the experiment is part of the PEBS<sup>1</sup> project, Work Package 2 Experimentation. The PEBS project is one of the “Small and Medium Projects” forming part of the FP7 Euratom programme. It is a multinational European research project that investigates processes affecting the engineered barrier performance of geological repositories for high-level waste disposal. The PEBS consortium consists of 17 leading nuclear research organizations, radioactive waste management agencies/implementing organizations, universities and companies.

### **1.2.2 Experiment development**

After the preparation of the design document (Aitemin, 2001) and the components procurement, the installation of the experiment was carried out in several steps. The instrumentation was installed from November 2001 to February 2002: in-rock pore pressure sensors, rock displacement sensors and some rock relative humidity sensors, canister displacement sensors, relative humidity sensors in bentonite and total pressure cells. The artificial hydration system was installed in March 2002. The installation of the experiment was finished in April 2002, including the retaining wall, the concrete plug and the data acquisition system.

---

<sup>1</sup> PEBS: Long-term Performance of Engineered Barrier Systems

The artificial hydration of the bentonite started in May 2002 and ended in June 2007. There was an initial hydration phase with an important amount of water injected (6,700 litres in two days) that was stopped after several water stains appeared on the wall. After that, the hydration was restarted and from September 2002 to June 2007, there were different hydration phases with continuous water injection. The detailed record of effective water inflow for bentonite hydration is included in report SDR EB N19 (Aitemin, 2007).

After the end of the hydration phase, the monitoring of the experiment continued in order to follow the evolution of the bentonite.

The Engineered Barrier Emplacement Experiment test is described in detail in the “EB Experiment Test Plan”, Project Deliverable 1, EC contract FIKW-CT2000-00017 (Aitemin, 2001), which includes the preliminary design, the emplacement and the operation.

BGR was in charge of performing at different stages of the EB experiment several geophysical and geotechnical oriented measurements for the characterization of the EBS, partly with subcontractors (TU Berlin, GMuG and Solexperts). For the initial characterization of the EB niche, immediately after the excavation, ultrasonic / seismic and geoelectrical measurements were performed in boreholes as well as along profiles (June 2001 – November 2001). After the closure of the niche (end of April 2002) and the start of the hydration phase (beginning of May 2002) a seismic long-term monitoring started (April 2002 – November 2003), including an acoustic emission experiment (April 2002 – April 2003). In November 2002 and one year later, in November 2003, geoelectrical measurements in the backfilled niche were conducted. The hydraulic characterization was executed in five stages between October 2001 and October 2003. These activities are documented in Schuster et al., 2004. In August 2011, more than nine years after the closure, BGR drilled two horizontal pilot boreholes for the characterization of the bentonite. Geophysical measurements (geoelectrical and ultrasonic), sampling of bentonite at different depths and preparations for a hydro test were done in August 2011 (Schuster et al., 2014). In July 2012 the seismic long-term monitoring was resumed in order to monitor the expected changes in rock and bentonite parameters during the dismantling process in winter 2012 (Schuster, 2014). This monitoring is ongoing. For the same reason a geoelectrical circular profile was reactivated and was used for daily measurements between September 2012 and May 2013 (this report).

### 1.3 Reactivation of an installed electrode array

To investigate the complex valued rock resistivity in the EB niche two annular profiles in the drift cross section and one horizontal profile along the drift axis were installed in 2001 (Kruschwitz & Yaramanci, 2002; Figure 5). After sealing the niche in 2001 the resistivity distribution was measured in two additional campaigns between November 2002 and November 2003 (Yaramanci & Siebrands, 2003). In July 2012 test measurement using these electrode arrays were performed successful. As an add-on to the seismic investigations (Schuster, 2014) it was decided to attend the dismantling procedure by a monitoring based on daily measurements using one annular profile.

Because of its add-on nature the work was originally not planned and so there was no adequate personal capacity for analyzing and interpretation of the huge amount of field data up to now. The results described in this report include only 3 of nearly 200 time steps, so there is potential for additional investigations.

## 2 Method

### 2.1 Fundamentals of DC Geoelectrics

To determine the spatial resistivity distribution (or its reciprocal – conductivity) in the ground, a direct current (DC) is introduced in the ground through two point electrodes (A,B).

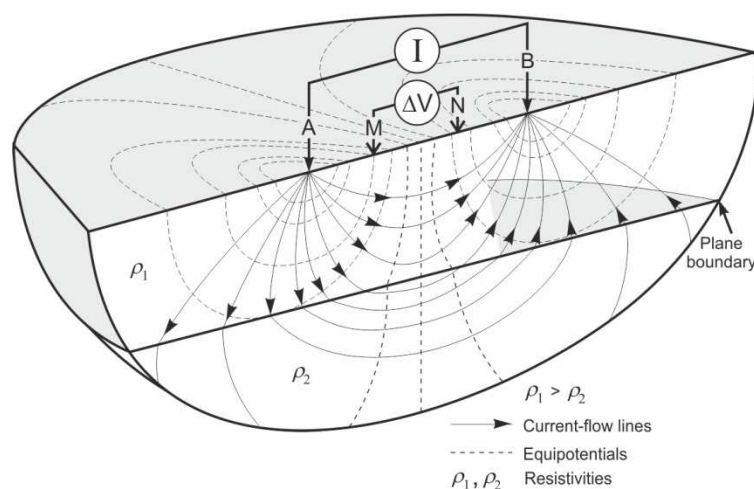


Figure 2: Principle of resistivity measurement with a four-electrode array (after Knödel et al., 2007)



The produced electrical field is measured using two other electrodes (M,N), as shown in Figure 2. A point electrode introducing an electrical current  $I$  will generate a potential  $V_r$  at a distance  $r$  from the source. In the case of a four-electrode array shown in Figure 2 consisting of two current electrodes (A,B) that introduce a current  $I$  and assuming a homogeneous half-space, the potential difference  $\Delta V$  between the electrodes M and N can be calculate as follows:

$$\Delta V = \rho I \left[ \frac{1}{2\pi} \left( \frac{1}{AM} - \frac{1}{AN} - \frac{1}{BM} + \frac{1}{BN} \right) \right]$$

$\overline{P_1 P_2}$  denotes the distance between two points  $P_1$  and  $P_2$ . Replacing the factor in square brackets by  $1/K$ , we obtain the resistivity of the homogeneous half space as follows:

$$\rho = K \frac{\Delta V}{I}$$

The parameter  $K$  is called configuration factor or geometric factor. For inhomogeneous conditions it gives the resistivity of an equivalent homogeneous half-space. For this value the term apparent resistivity  $\rho_a$  is introduced, which is normally assigned to the center of the electrode array. Multi-electrode resistivity meters enable the measurement of 2D resistivity surveys (2D imaging). The advantages of this kind of measurements are their high vertical and horizontal resolution along the profile. Figure 3 shows a commonly used setup of a Wenner- $\alpha$  configuration. All electrodes are placed equidistantly (distance  $a$ ) along a profile. The configuration factor for this special configuration is given by  $K = 2\pi a$ . The diagram displaying the apparent resistivity as a function of location and electrode spacing is called pseudosection and provides an initial picture of the resistivity distribution. Other commonly used arrays are Schlumberger, dipole-dipole, Wenner- $\beta$  (a special dipole-dipole configuration) or pole-dipole. The Wenner- $\alpha$  configuration is a good compromise between spatial resolution on the one hand and the signal-to-noise ratio on the other hand. In case of full-space conditions, the geometric factor is multiplied by a factor of 2.

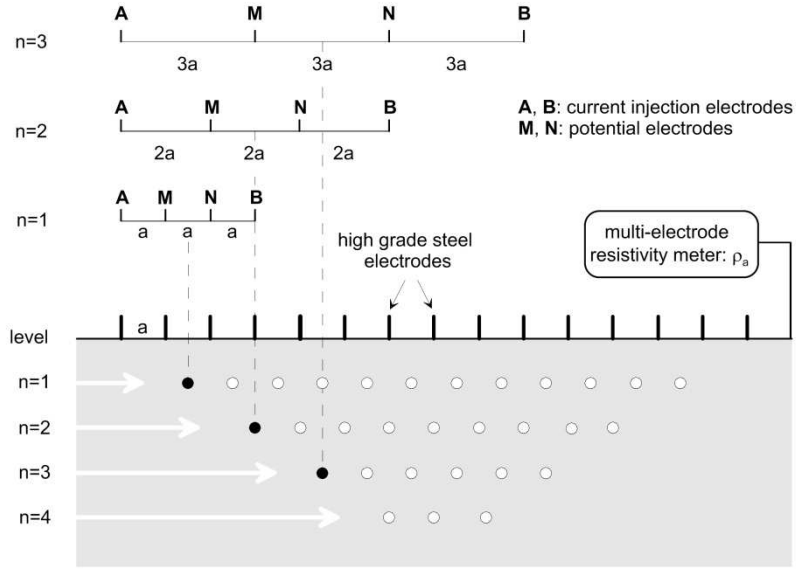


Figure 3: Setup for a 2D resistivity measurement (imaging) using a Wenner- $\alpha$  electrode configuration and presentation as a pseudosection (modified after Knödel et al., 2007)

## 2.2 Inversion

An inversion process of the measured data is necessary for the final interpretation. This process transforms the apparent resistivities into a reliable model discretized into a distinct number of elements of homogeneous resistivity. Mathematical an inversion algorithm minimizes iteratively the data functional defined by (see Günther et al., 2006)

$$\Phi_d(\mathbf{m}) = \|\mathbf{D}(\mathbf{d} - \mathbf{f}(\mathbf{m}))\|_2^2 - \lambda \|\mathbf{C}(\mathbf{m} - \mathbf{m}^0)\|_2^2$$

with

- the vector of logarithms of N single data  $\mathbf{d} = (\log(\rho_1^a), \log(\rho_2^a), \dots, \log(\rho_N^a))^T$
- the vector of logarithms of M single model parameters  $\mathbf{m} = (\log \rho_1, \log \rho_2, \dots, \log \rho_M)^T$
- the model response  $\mathbf{f}(\mathbf{m})$
- the vector of logarithms of M single start model parameters  $\mathbf{m}^0 = (\log \rho_1^0, \log \rho_2^0, \dots, \log \rho_M^0)^T$

- the weighting matrix  $\mathbf{D} = \text{diag}(1/\varepsilon_i)$  ( $\varepsilon_i$  is the associated error of the data point  $\rho_i^a$ )
- the constraint matrix  $\mathbf{C}$
- the regularization parameter  $\lambda$

The logarithms are used to ensure positivity of all resistivities. The forward operator is generally obtained by finite-difference (FD) or finite-element (FE) methods (Rücker et al., 2006). All inversions are performed using the non-commercial software BERT (Boundless Electrical Resistivity Tomography) developed by Th. Günther<sup>2</sup> and C. Rücker<sup>3</sup>. BERT allows the consideration of any geometry (2D, 3D, topography, bounded/unbounded, electrode shapes,...) and provides full control of the whole inversion process.

### 3 Field Measurements

#### 3.1 Hardware and setup

The measurements were performed using a *4 point light hp* device of *Lippmann Geophysikalische Messgeräte* in combination with a multiplexer consisting the electrode units. The electrical contact to the special plug of the installed multicore cable was performed using an interface box. Figure 4 shows the experimental setup. The device was normally controlled by the software *GeoTest* of *Geophysik – Dr. Rauen*. A monitoring mode within the 4 point light device enables autonomous measurements without a computer for several weeks, but there was the need for manual data readout.

---

<sup>2</sup> Leibniz Institute of Applied Geophysics, Hannover

<sup>3</sup> Technical University of Berlin, Department of Applied Geophysics



Figure 4: Pictures of the experimental setup; left: test measurement, laptop controlled; right: installation in an aluminum box for monitoring, device controlled

### 3.2 Monitoring period

The geoelectrical monitoring covers the period between September 27<sup>th</sup>, 2012 and May 24<sup>th</sup>, 2013 by a daily measurement, 240 data sets in all. Because of cable destruction while dismantling at two times there exist two periods of unusable data sets:

- between 27.11.2012 and 17.12.2012 (21 days)
- between 13.01.2013 and 07.02.2013 (26 days)

For the last period after February 7<sup>th</sup> the connection to four electrodes (# 15, 16, 22, 27) was lost permanently (see Figure 14).

### 3.3 Layout

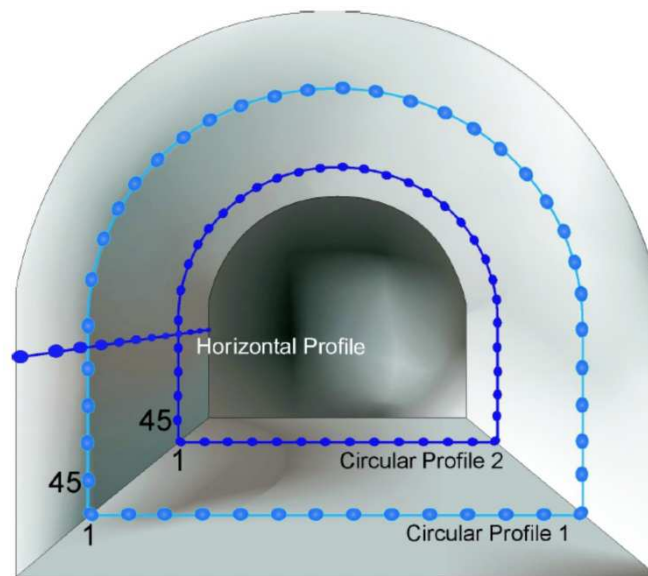


Figure 5: Sketch of the three electrode profiles installed in the EB niche in 2001 (Kruschwitz & Yaramanci, 2002)

After excavation of the EB niche three electrode profiles were installed in 2001 (Figure 5), one horizontal profile at the left wall and two circular profiles in a distance of 2.65 m and 3.65 m to the face of the niche, respectively. The 45 electrodes of the circular profiles located every  $8^\circ$  (measured from a central point of the niche), what almost corresponds 21 cm while the electrode distance of the horizontal profile is 12.5 cm. The installations were used to investigate the change of resistivity distribution due to the stress relaxation in the Opalinus Clay in three campaigns (Kruschwitz & Yaramanci, 2002). After emplacement of the canister, filling the excavation and closing the niche with a concrete plug, two additional measurements were performed in 2002 (Yaramanci & Siebrands, 2003).

In July 2012 a first test measurements were performed to reactivate these old installations. This test was successful, all electrodes were accessible showing contact resistances between  $50 \Omega$  and  $2 \text{ k}\Omega$  (see Figure 6). The regions concrete floor/bed and Opalinus Clay can be clearly distinguished by the resistance level. For technical reasons only one of the profiles could be used for a monitoring measurement. Since only the circular profiles provide 2D information it was decided to use the circular profile 2 because of its lower distance to the face of the niche.

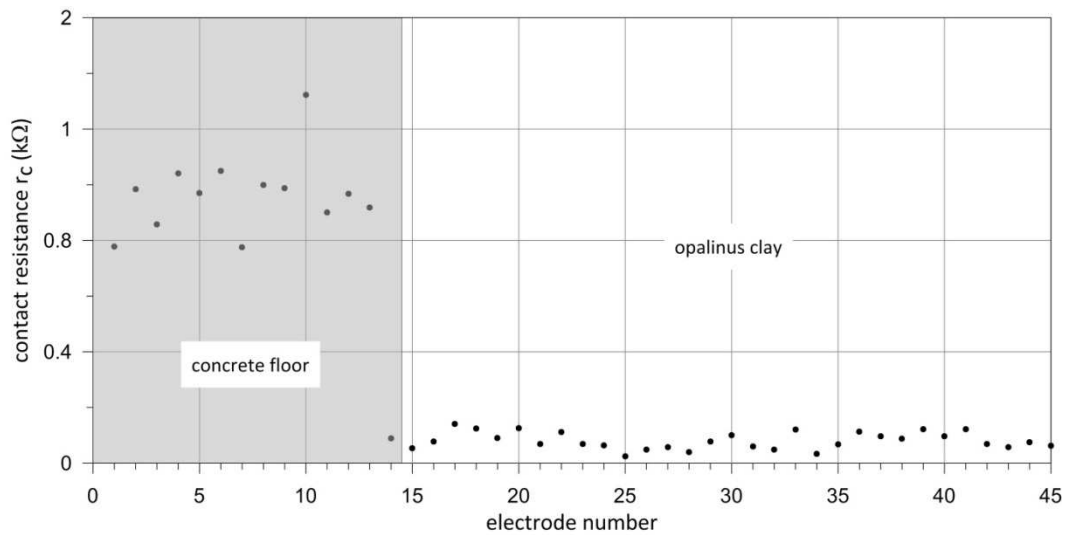


Figure 6: Contact resistances of all electrodes of circular profile 2 on July 4<sup>th</sup>, 2012

### 3.4 Configurations and inversion

Figure 7 shows the geometry of the niche, the position of the electrodes and the outlines of the concrete bed, the bentonite blocks and the dummy canister.

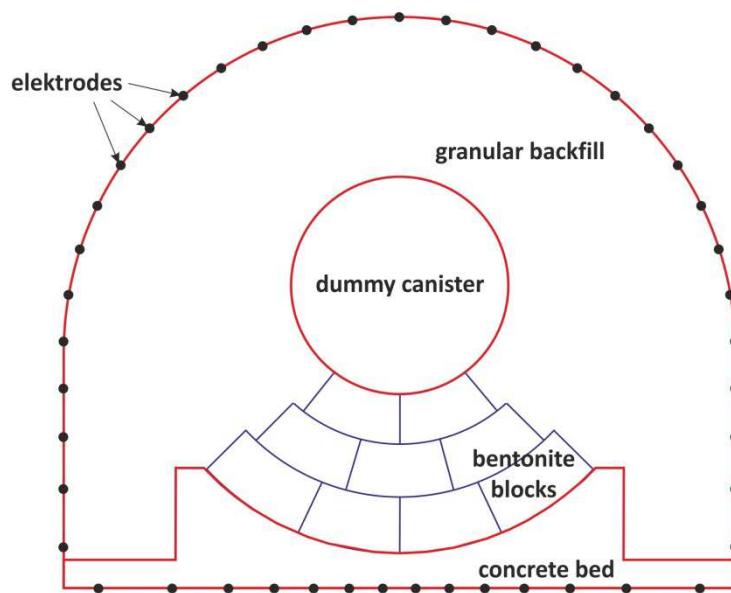


Figure 7: Geometry of EB niche including concrete bed and dummy canister with electrode positions

Because the measurement of ring profiles is not implemented as a standard type in the operation software of the device, a custom configuration file was created consisting all possible Wenner- $\alpha$  configurations (630 single measurements), all possible Wenner- $\beta$  configurations (630 single measurements) and 630 additional measurements in dipole-dipole configuration. Until now only the Wenner- $\alpha$  measurements are used for the inversion because of their highest configuration factors and the highest signal to noise ratio.

The main points for the inversion of distinct time steps are:

- Geometry: 2D full scale
- Used configurations: 630 single measurements (resistance values) in Wenner- $\alpha$  configuration
- Configuration factors: built by BERT using the given electrode positions
- Input of a priori information: outlines of niche, concrete bed and dummy canister (all red lines displayed in Figure 7), at these lines arbitrary contrasts are allowed
- Start model: homogeneous with  $\rho_{\text{start}}=4.25 \text{ } \Omega\text{m}$  (mean value of all considered measurements)

## 4 Results and Conclusion

### 4.1 Situation before dismantling operation

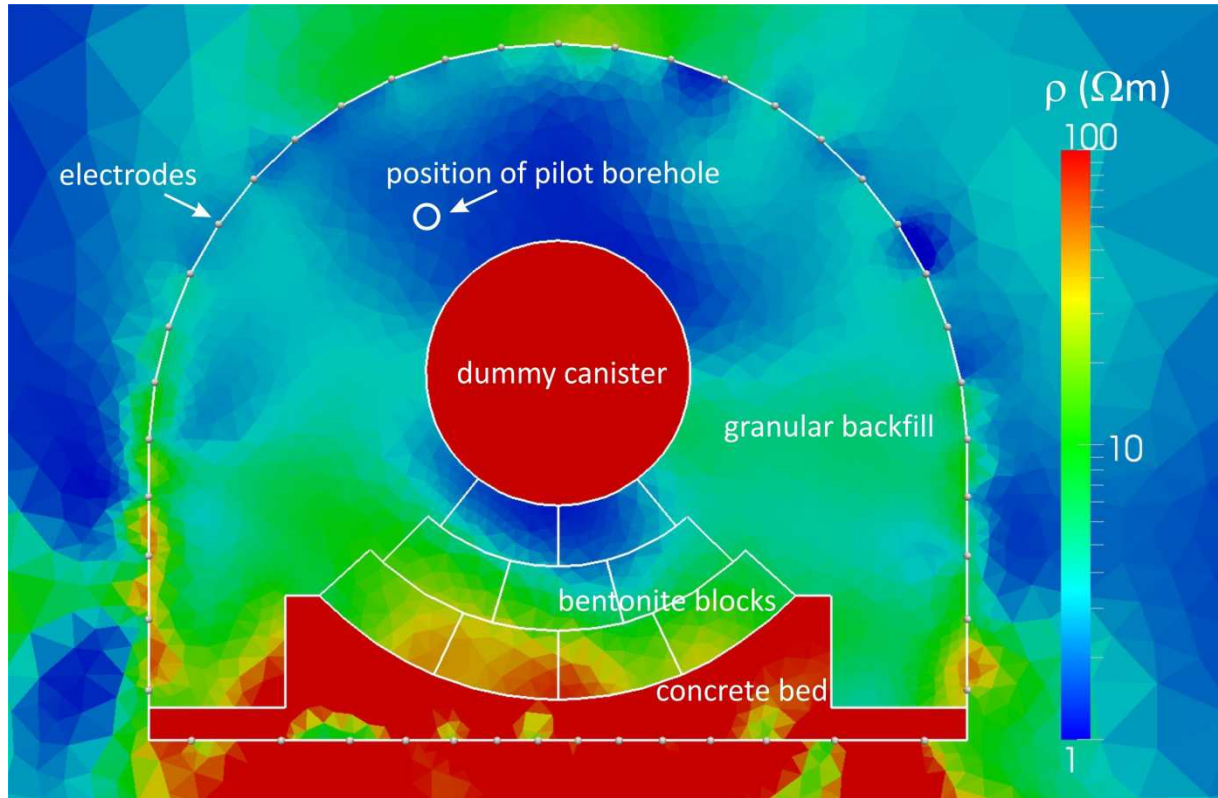


Figure 8: Model of the spatial resistivity distribution on September 30<sup>th</sup> 2012

Figure 8 shows the model of the spatial resistivity distribution on September 30<sup>th</sup> 2012, about 3 weeks before start of dismantling operation. The main structures of this undisturbed state are:

- The concrete floor and bed are resolved as high resistive structures with more than 100  $\Omega\text{m}$  as expected.
- The dummy canister is also reconstructed as a high resistive area ( $>> 100 \Omega\text{m}$ ), because the lacquer coat and the textile membrane that surrounds the canister prevent the current flow from entering the canister's steel mantle.
- The lowest resistivities (below 3  $\Omega\text{m}$ ) are displayed above and directly below the canister.



- There is only a small variability of resistivity seen in the horizontal direction within the bentonite, but there is obviously a vertical gradient present with higher resistivities ( $\sim 10 \Omega\text{m}$ ) at the floor.
- No contrast can be seen at the border between the bentonite blocks and the granular material.

The input of the outlines of the canister and the concrete bed effect the building of a high resistivity contrast while the resistivity contrast at the outline of the niche is very small.

#### 4.1.1 Comparison with results from pilot borehole

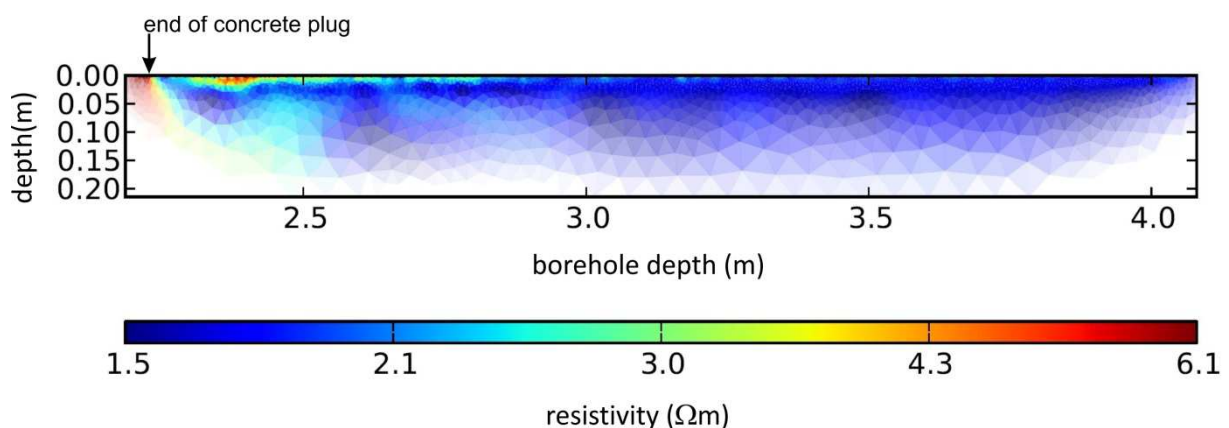


Figure 9: Result of the geoelectrical profile measurements in the pilot borehole

As a check of the reconstructed resistivity range the modelled resistivity is compared to a result of a geoelectrical measurement in a pilot borehole, which was drilled in August 2011 (Schuster et al., 2014). The position with respect to the section is displayed in Figure 8.

Figure 9 shows the inversion result of the borehole measurements performed in 2011. At a borehole depth of about 2.2 m the end of the concrete retaining wall is seen as a high resistive zone. In the range of 2.3 m and 2.8 m a small zone ( $\sim 2\text{--}3 \text{ cm}$ ) of higher resistivities is visible directly at the borehole wall which can be interpreted as an indication of a Borehole Disturbed Zone (BDZ) due to the drilling process. For the deeper part of the borehole the resistivity distribution is very homogeneous with values about  $1.7 \Omega\text{m}$ . This result agrees to the resistivity values shown in Figure 8 at this position.

#### 4.1.2 Comparison with results from sample analysis

The undisturbed resistivity pattern can be compared to results of sample analysis performed on site in different sections vertical to the niche axis. Figure 10 shows the position of the geoelectrical profile 2 with respect to the different sampling sections performed by Aitemin (Palacios et al., 2013).

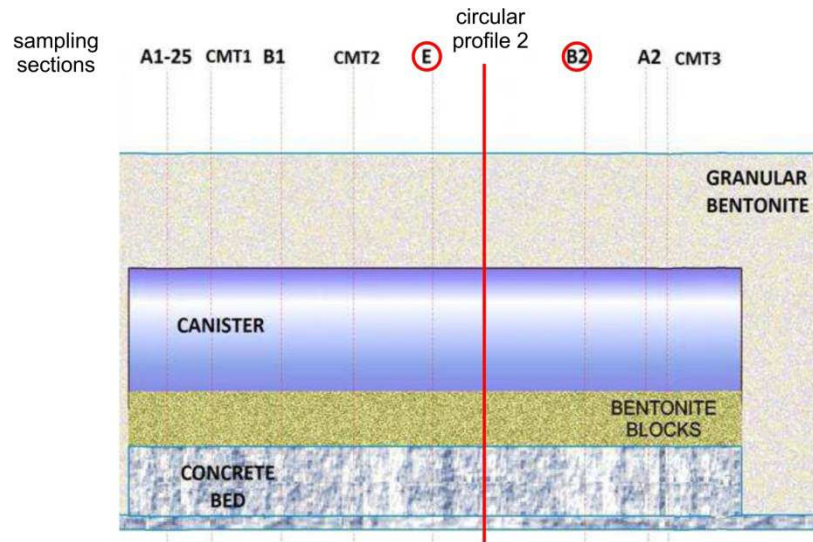


Figure 10: Position of sampling sections and the used circular profile

The sections “E” and “B2” are the nearest neighbors to the geoelectrical section. In Figure 11 the spatial distributions of the measured water content (%) at the sections “E” and “B2” are displayed.

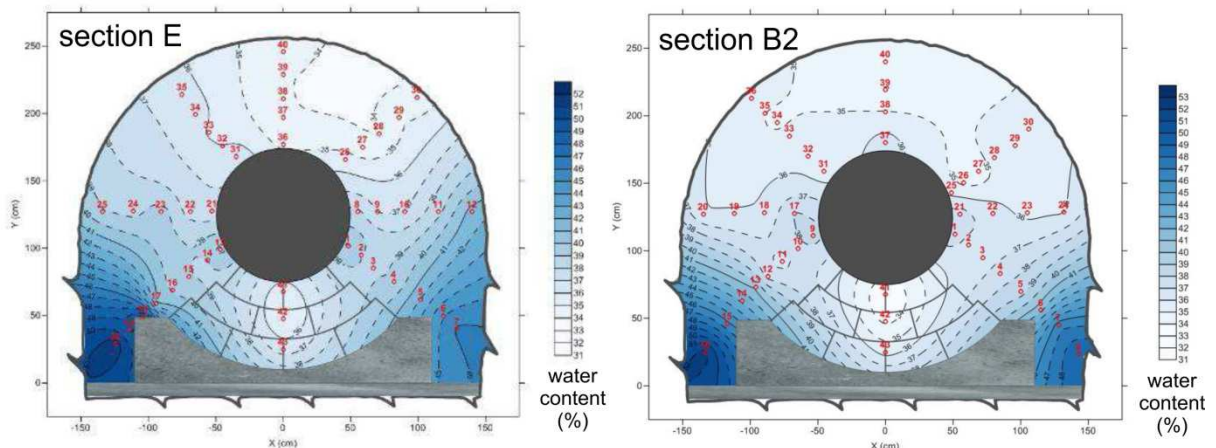


Figure 11: Spatial distribution of water content at section “E” and “B2” as a result of sample analysis while dismantling (from Palacios et al., 2013)

The distinct sampling points are oriented in 8 radial lines with varying angle and displayed as red circles. The distributions of both sections are very similar. The main structures are:

- The lowest water contents were measured above and directly below the canister.
- Very small horizontal variations are visible, while a strong vertical gradient can be observed in the vertical direction with the highest water content in the left and right corners, respectively.
- There is no indication visible for a contrast between block and granular material

Overall, the structures observed for the water content and the electrical resistivity look very similar. However, the correlation with lower resistivities at regions of lower water content is anomalous because most sediments show an opposite correlation. To investigate this behavior 6 samples of section “E” were analyzed in the BGR laboratory by S. Kaufhold.

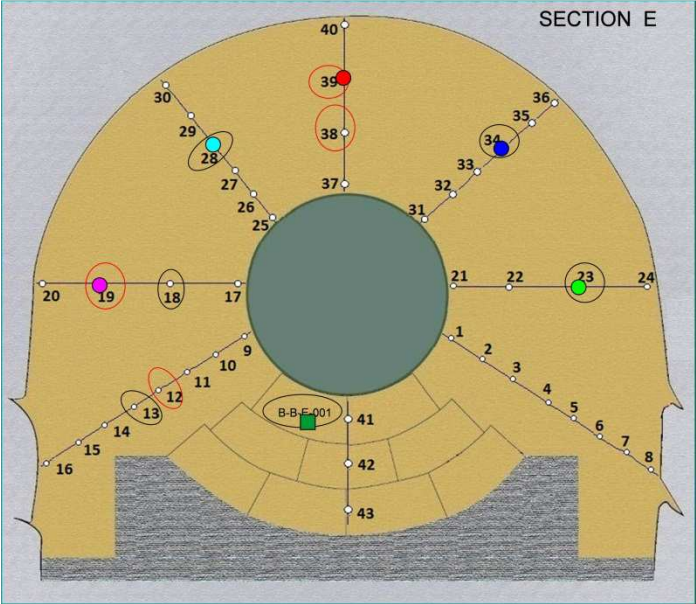


Figure 12: Positions of samples (section “E”) for laboratory investigations

In Figure 12 the sampling positions are displayed. 5 samples consist of the granular backfill material indicated as colored circles while one sample is part of a bentonite block (indicated by a green rectangle) located directly below the canister.

In a first step, all samples were fully saturated. During the drying process at free air the resistivity was measured at different stages of water content. The results are compiled in Figure 13 as curves of electrical resistivity as a function of water content. All curves show a clear trend to higher resistivities at higher water contents independent of the material origin. It is a special property of the used bentonite material.

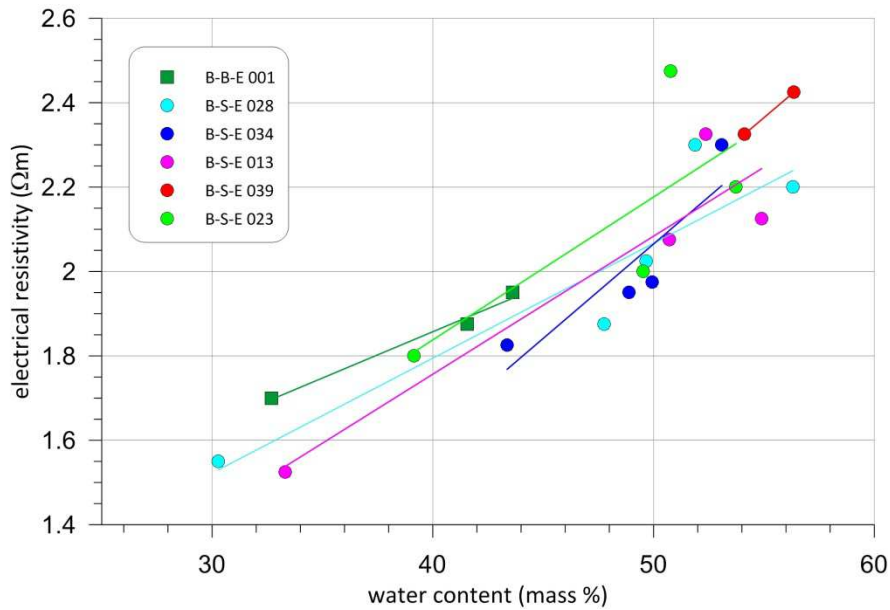


Figure 13: Resistivity as a function of water content of 6 bentonite samples

This result confirms the in situ observed positive correlation between electrical resistivity and the water content of the material.

#### 4.2 Situation after finished dismantling operation

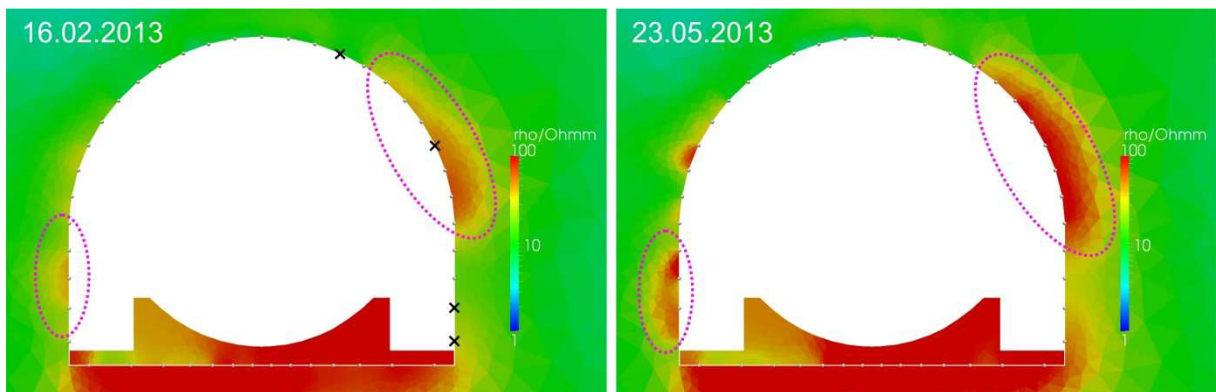


Figure 14: Resistivity distribution in the Opalinus Clay around the EB niche at 2 distinct time steps after finished dismantling; left: February 16<sup>th</sup> 2013, right: Mai 23<sup>th</sup> 2013

Figure 14 shows the spatial resistivity distribution in the Opalinus Clay around the EB niche at 2 distinct time steps after finished dismantling. The left image displays the situation at February 16<sup>th</sup> 2013 (the black crosses denote the lost electrodes, cf. section 3.2) while the right picture displays the situation about 3 month later. The concrete floor and the remaining concrete bed are still high resistive structures. In February the region around the niche is

characterized by resistivities of about  $10 \Omega\text{m}$ , except of two regions (right top and left wall down, denoted by dashed magenta ellipses) where higher resistivities ( $>40 \Omega\text{m}$ ) are visible. Three month later these regions increase in extension as well as in resistivity contrast. Between the electrodes 38 and 39 an additional zone of increased resistivity is now visible.

#### 4.2.1 Comparison to a stress analysis

Figure 15 shows the spatial stress distribution as a result of a stress analysis of the EB niche before emplacement (Corkum, 2006). There exist broad areas of low confining stress at the left top and the bottom of the niche. But remarkable are the two red zones indicating areas of high deviatoric stress exactly at the positions where the geoelectrical measurements show the enhanced resistivities.

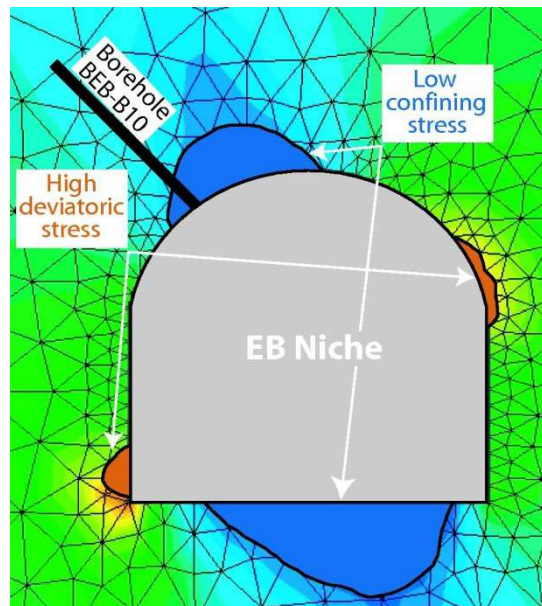


Figure 15: Spatial stress distribution in the environment of the EB niche (Corkum, 2006)

After the stress relaxation after dismantling the niche this high deviatoric stress could enforce the formation of micro cracks in the Opalinus Clay. These cracks may lead to higher drying out at this positions and results finally in a higher electrical resistivity.

## 5 Summary

A previous to the canister emplacement installed circular electrode profile was reactivated for monitoring the dismantling process in the EB niche by daily geoelectrical measurements.

Under undisturbed conditions without influences of dismantling the inverted spatial resistivity distribution provides an image of the homogenization of the bentonite material due to the active saturation. An anomalous positive correlation between electrical resistivity and water content (result of on-site sample analysis while dismantling procedure) can be observed. Further laboratory measurements of bentonite samples confirm this correlation.

In the resistivity models of two time steps after finished dismantling two zones of higher resistivity can be observed. The extension and the absolute resistivity values increase with time. As a result of a local stress analysis of the EB niche there are located areas of high deviatoric stress at the same positions. The resistivity image shows the effect of the stress distribution building EDZ structures after dismantling the niche.

## **Acknowledgements**

We thank C. Czora, H. Albers (both BGR) and T. Theurillat (Swisstopo) for the technical support of the work on-site. The interface box was provided by S. Braun (TU Berlin). Many thanks to B. Palacios (Aitemin) for providing the 6 bentonite samples and S. Kaufhold (BGR) for carrying out the laboratory measurements.

## **6 References**

Aitemin (2001): Engineered Barrier Emplacement Experiment in Opalinus Clay “EB” Experiment. TEST PLAN. Madrid, 76 pp.

Aitemin (2007): Engineered Barrier Emplacement Experiment in Opalinus Clay “EB” Experiment. Sensors data report N° 19 and Mont Terri TN2007-11. Period 22/11/2001 to 30/06/2007, 38 pp.

Corkum, A. G. (2006): Non-Linear Behaviour of Opalinus Clay Around Underground Excavations. University of Alberta, p. 206.

Günther, T., Rücker, C. & Spitzer, K. (2006): Three-dimensional modeling and inversion of dc resistivity data incorporating topography – II. Inversion. – *Geophys. J. Int.* **166**: 506–517.

Knödel, K., Lange, G. & Voigt, H.-J. (2007): Environmental Geology – Handbook of Field Methods and Case Studies: 1357 S., 501 Abb., 204 Tab.; Berlin (Springer) – ISBN 978-3-540-74669-0

Kruschwitz, S. & Yaramanci, U. (2002): Engineered Barrier (EB) Experiment: EDZ Geophysical Characterization. Detection and Characterization of the Disturbed Rock Zone in Claystone with Complex Valued Geoelectrics, Mont Terri Rock Laboratory – Technical Report 2002-01,

Palacios, B., Rey, M., Garcia-Sinerez, J. L., Villar, M. V., Mayor, C & Velasco, M. (2013): Engineered Barrier Emplacement Experiment in Opalinus Clay “EB” Experiment. As-built of dismantling operation. PEBS Deliverable D2.1-4

Rücker, C., Günther, T. & Spitzer, K. (2006): Three-dimensional modelling and inversion of dc resistivity data incorporating topography – I. Modelling. – Geophys. J. Int. **166**: 495–505.

Schuster, K., Alheid, H.-J., Kruschwitz, S., Siebrands, S., Yaramanci, U., Trick, T., Manthei, G. (2004), Observation of an Engineered Barrier Experiment in the Opalinus Clay of the Mont Terri Rock Laboratory (CH) with Geophysical and Hydraulic Methods, 2 posters and abstract, Euradwaste'04, Radioactive waste management - Community policy and research initiatives, Sixth European Commission Conference on the Management and Disposal of Radiactive Waste, 29. March - 1. April 2004, Luxembourg.

Schuster, K. (2014): Engineered Barrier Emplacement Experiment in Opalinus Clay “EB” Experiment. Seismic Long-term Monitoring of EDZ Evolution. PEBS Deliverable D2.1-6.

Schuster, K., Furche, M., Schulte, F., Tietz, T., Sanchez Herrero, S., Velasco, M., García-Sineriz, J.-L., Gaus, I., Trick, T., Mayor, C. (2014): Engineered Barrier Emplacement Experiment in Opalinus Clay “EB” Experiment. EBS Pilotboreholes – sampling, geophysical and geotechnical measurements. PEBS Deliverable D2.1-1.

Yaramanci, U. & Siebrands, S. (2003): Geoelectrical Characterization of the Disturbed Rock Zone in the Underground Rock Laboratory “Mont Terri”, TU Berlin, Department of Applied Geophysics, Internal report